Minibeam radiation therapy at a conventional irradiator: dose-calculation engine and first tumor-bearing animals irradiation

W. González[a], M. dos Santos[a], C. Guardiola[a], R. Delorme[a], C. Lamirault[a], M. Juchaux[a], M. Le Dudal[b,c], G. Jouvion[b,c], Y. Prezado[a,*]

[a] *IMNC-UMR 8165, CNRS; Paris 7 and Paris 11 Universities, 15 rue Georges Clemenceau, 91406 Orsay Cedex, France*
[b] *Institut Pasteur, Experimental Neuropathology Unit, Department of Global Health, 75015 Paris, France*
[c] *Histologie, Embryologie et Anatomie Pathologique, Ecole Nationale Vétérinaire d'Alfort, Université Paris-Est, Maisons-Alfort, France*

Abstract

Purpose: Minibeam radiation therapy (MBRT) is a novel therapeutic strategy, whose exploration was hindered due to its restriction to large synchrotrons. Our recent implementation of MBRT in a wide-spread small animal irradiator offers the possibility of performing systematic radiobiological studies. The aim of this research was to develop a set of dosimetric tools to reliably guide biological experiments in the irradiator.
Methods: A Monte Carlo (Geant4)-based dose calculation engine was developed. It was then benchmarked against a series of dosimetric measurements performed with gafchromic films. Two voxelized rat phantoms (ROBY, computer tomography) were used to evaluate the treatment plan of F98 tumor-bearing rats. The response of a group of 7 animals receiving a unilateral irradiation of 58 Gy was compared to a group of non-irradiated controls.
Results: The good agreement between calculations and the experimental data allowed the validation of the dose-calculation engine. The latter was first used to compare the dose distributions in computer tomography images of a rat's head and in a digital model of a rat's head (ROBY), obtaining a good general agreement. Finally, with respect to the in vivo experiment, the increase of mean survival time of the treated group with respect to the controls was modest but statistically significant.
Conclusions: The developed dosimetric tools were used to reliably guide the first MBRT treatments of intracranial glioma-bearing rats outside synchrotrons. The significant **tumor response** obtained with respect to the non-irradiated controls, despite the heterogenous dose coverage of the target, might indicate the participation of non-targeted effects.

Keywords: X-ray Minibeam radiation therapy, Monte Carlo simulations, ROBY

*Corresponding author at: IMNC-UMR 8165, CNRS; Paris 7 and Paris 11 Universities, 15 rue Georges Clemenceau, 91406 Orsay Cedex, France
Email address: prezado@imnc.in2p3.fr (Y. Prezado)

1. Introduction

Minibeam radiation therapy (MBRT) is an innovative tumor therapy that was initiated at synchrotrons [1].

The dose is spatially fractionated by summing submillimetric (500–700 μm) beams in a comb-like pattern: the dose profiles consist of peaks and valleys with high doses in the beam path and low doses in the spaces between them [2]. The peak-to-valley dose ratio (PVDR) is considered an important dosimetric parameter [3], since in order to spare the normal tissues, high PVDR and low valley doses are required. MBRT has been shown to increase normal tissue tolerances [4]. In addition, a significant delay in tumor growth was observed in glioma bearing rats [5].

The extension of MBRT to contexts outside of synchrotron biomedical beamlines towards a conventional irradiator would facilitate the realization of comprehensive radiobiological studies [6]. For that purpose, we have modified a commercial X-ray small animal irradiator to make it suitable for MBRT small animal irradiation [6]. This involves obtaining minibeam patterns with comparable widths and PVDR values to those at synchrotrons. This strategy offers several advantages over synchrotron radiotherapy (RT), such as reduced costs, and the possibility of envisioning clinical trials with modified equipment, without the difficulties imposed by the scarce beam time at synchrotrons.

The aim of this research was to develop the necessary dosimetric tools to design, guide, and interpret biological experiments. This included the development of a Monte Carlo-based dose calculation engine, to guide and analyse small-animal MBRT experiments. Calculations in a voxelized rat brain, both using and comparing an analytical phantom (ROBY) and computer tomography images of the rat to be treated, were performed. The suitability of using ROBY in case computer tomography images (CT) of the animals are not available, was established. The developed dosimetry tools were used to guide the first evaluation of the effectiveness of **tumor response** in glioma-bearing rats outside synchrotron sources, which is also reported. To the best of our knowledge, this is the first proof-of-concept of MBRT irradiation of intracranial gliomas in rodents performed in a table-top system.

2. Materials and Methods

2.1. Monte Carlo simulations

The implementation of the MBRT technique was carried out at the Small Animal Radiation Research Platform (SARRP, XSTRAHL Ltd., UK) [7] available at the Experimental Radiotherapy Platform of the Curie Institute in Orsay (France). The SARRP was modified to make it suitable for MBRT experiments [6]. The SARPP can be used both for therapy and imaging. A small focal spot (1 mm diameter) leading to energies around 60-70 kVp are used for imaging, while higher kV X-ray tension and a larger focal spot (5.5 mm diameter) are used for irradiations. The collimator was designed to obtain beam widths and centre-to-centre (ctc) distances comparable to those previously used at ESRF (600 μm width and 1200 μm ctc) [6].

Monte Carlo (MC) simulations were used to guide the design, setup optimization and to develop a Monte Carlo-based dose calculation engine. The MC toolkit Geant4 version 10.01 [8] was employed. For all the particles, a cut energy of 250 eV was considered. The Livermore electromagnetic physics list was used.

2.1.1. Virtual source model

A virtual source was defined to save computing time. For source definition, MC simulations were split into two parts. First, electron interactions on the tungsten anode were simulated and the phase space variables (particle type, energy, position, momentum) of the photon created, after passing through the inherent and additional filtration of 0.8 mm of berilium and 0.15 mm of copper, were saved into a phase space file (PSF). The analysis of the information contained in this PSF was then used to generate a photon virtual source model placed at the anode position of the SARRP. For fine tuning of the source, an iterative process guided by the comparison of the simulated and measured dose distributions was followed. The energy spectrum was determined by using the sofware SpekCalc [6]

The criteria of acceptability for the dose calculations compiled in the Technical Report Series 430 (TRS 430) of the International Atomic Energy Agency [9] were considered.

The validated source model was then used as input for the subsequent dose calculations.

2.1.2. Dose calculation engine

A Geant4-based dose engine (dose-engine) for X-ray MBRT was developed using the idea of the manipulation of a voxelized phantom from the Geant4 extended example DICOM. The DICOM example shows how to construct a geometry in Geant4 starting from the CT of real patient data [8].

The number of primary particles used in the simulations was 10^{11} so that the global uncertainty was 2%, with a coverage factor $k = 1$. The dose was scored in voxels of 0.1 x 0.1 x 0.1 mm^3 in four different phantoms. In order to speed up the calculation a nested parametrization was employed.

Two phantoms with dimensions of 200 x 200 x 40 mm^3, mimicking those used in the experimental measurements, were considered. One of them was a homogenous solid water phantom (Gammex [10]). It was used for comparison with the experimental dosimetry data to fine-tune the geometric characteristics of the collimator, as well as to benchmark our dose-engine. The other one, a heterogeneous phantom, consisting of a 10-mm thick slab of bone and three 10-mm thick slabs of solid water was employed to validate the performance of the dose-engine in the presence of heterogeneities.

Two voxelized rat phantoms were used to plan the dosimetry of the radiotherapy treatment of the tumor lesions on the head. The first one, called ROBY [11], is a digital model of the rat's whole body. Similar digital phantom has been used in previous RT studies [12]. In this study, we only considered the slice of the ROBY phantom representing the rat's head. The second phantom was composed of the CT images of a 7-week old rat. The CT images were acquired using the SARRP. The reconstruction was done by filtered Backprojection without post filtering. The figure 1 represent a sagittal section of the CT phantom including the beam eye view of the arrangement projected over it.

Regarding the ROBY phantom, the attenuation coefficient table as a function of the energy was used to generate the voxelized geometry. In our case, for each energy, the values of the attenuation coefficient were replaced by the material's density. Using a customized precompilation routine, the raw output file of ROBY was converted into 300 slices with dimensions of 55.3 x 35.6 x 0.1 mm^3.

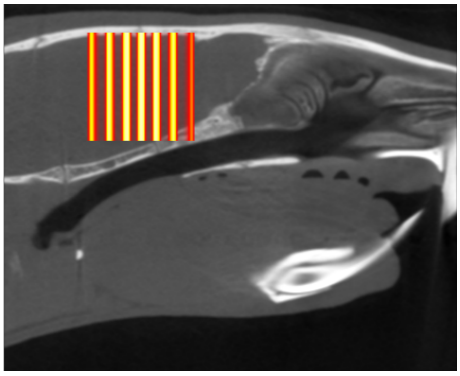

Figure 1: Beam eye view image of the beam arrangement projected on a sagittal section of the CT phantom.

Concerning the CT images, the conversion from Hounsfield units (HU) per pixel to material density was performed following the steps described by Reynaert et al. [13]. Using the pre-compiled routine, 300 slices with dimension 68.1 x 41.1 x 0.1 mm^3 were generated.

The dose distribution in the rats' brains in the in vivo experiment were assessed by using the developed dose-engine.

A comparison between the dose distributions obtained in ROBY and in the rat's CT was performed to evaluate whether ROBY could be used as a substitute to plan experiments. This could be convenient if the sizes of the animals of the same group are not very homogeneous and there is no possibility of performing high-resolution CT for each of the animals to be irradiated, a procedure that is very time consuming. The advantage of ROBY is that the dimensions can be modified to be adapted to different ages/sizes of the rats to be irradiated.

2.2. Experimental dosimetry

The experimental dosimetry was performed following the 'two-step' protocol developed for synchrotron MBRT [2]. In this protocol, the reference dose (Dref) is measured in a broad beam configuration with a thimble ionization chamber (PTW PinPoint 31016 chamber). A reference field size of 40 x 40 mm^2 was chosen.

For relative dosimetry, radiochromic films (Gafchromic EBT3 films, Gafchromic^{TM}) were used. A flatbed scanner (Epson Perfection V750-M Pro Scanner) served to readout the films, following the method described in Devic et al. [14]. Film handling was carried out taking into account the recommendations provided by Task Group 55 of the American Association of Physics in Medicine (AAPM) [15]. The uncertainties of the film dose measurements were evaluated following the method described in Sorriaux et al. [16]. The main contributions to the overall uncertainty come from the determination of the absolute dose with the ionization chamber (2%), the measurement of the film's optical density (0.5%), film calibration (1.5%), and the mean standard deviation of the average dose in the peak and valley regions (2%). The overall uncertainty amounted to 3.2%. To incorporate other possible sources of uncertainty, a conservative value of 4% was used.

The films were placed at different depths in two different plastic phantoms (Gammex [10]). The first one was a solid water phantom consisting of 4 slabs with dimensions of 200 x 200 x 10 mm^3. The second one was a heterogeneous phantom composed of 1 slab (200 x 200 x 10 mm^3) of bone-equivalent material and 3 slabs of solid water.

Percentage depth dose curves and lateral dose profiles were measured. Finally, the output factors were assessed by comparing the ratio of the dose measured by the films irradiated with a 40 x 40 mm^2 field size and those irradiated with MBRT at different depths.

2.3. In vivo experiment

The dosimetry tools developed were used to guide the first evaluation of **tumor response** effectiveness in glioma-bearing rats. The ethical guidelines of our institutions for animal welfare were followed in conducting the experiments. They were approved by the Ethics Committee of the Institut Curie and the French Ministry of Research (permit no. 6361-201608101234488).

A number of 10000 F98 rat cells (ATCC® CRL-2397^{TM}), transfected with the luciferase gene, were implanted in male Fischer 344 rats (Janvier Labs). The cells were innoculated, as in our previous research [17]. Bioluminescence Imaging (BLI) at an IVIS spectrum (PerkerElmer) was carried out to confirm the presence of a tumor. A double control was performed through a histopathological analysis when the animals died.

Two groups of animals (7 weeks old at the moment of irradiation) were considered: i) a control group (tumor bearing rats, non-irradiated) ($n = 4$); ii) a group of tumor-bearing rats $n = 7$) that received MBRT.

The rats were irradiated 11 days after implantation. The irradiation was a lateral one from left to right. In this irradiation configuration, the centre of the tumor was located at a depth of approximately 16 mm. The dose delivered was 58 Gy (peak dose) as measured at 1 cm in depth in a water phantom. The goal was to assess whether some **tumor response** is achieved with those high doses in MBRT.

The dose distributions in the rat's brain were calculated with the dose engine described in section 2.1.2, and will be presented in the Results section. The doses were delivered in only one fraction.

3. Results

In this section we present the dose measurements, the benchmarking of the dose-engine, and the dose calculations to plan the in vivo experiment. The results of this first evaluation of the effectiveness of MBRT for glioma **tumor response** in a conventional irradiator will also be presented.

3.1. Dosimetry

As explained in the Methods section, a virtual source model placed at the anode position was extrapolated from the dose distributions measured in standard conditions (seamless irradiation) by using an iterative method. A Gaussian source with a full width at half maximum (FWHM) of 2.3 mm and a divergence of 20 degrees reproduced well the experimental data. Figure 2 shows the transversal dose profiles for a seamless irradiation (40 x 40 mm^2 field size).

A good agreement between the MC simulations and the experimental data is observed, according to the criteria explained in the TRS430 [9]. The relative differences around the maximum region of the transverse dose profiles were 2% at most. The difference regarding the penumbra distances between simulated and experimental profiles was smaller than 1.2 mm.

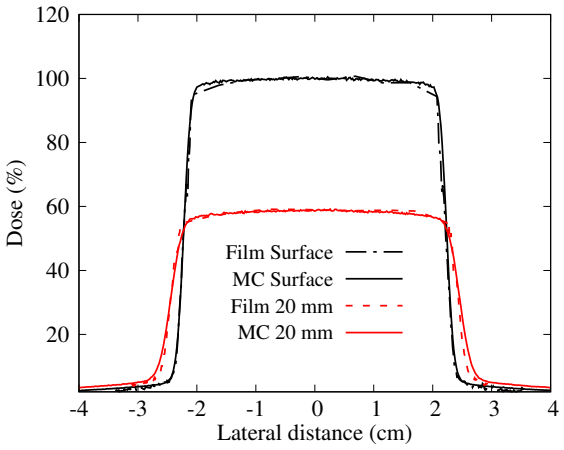

Figure 2: Comparison of experimental and calculated doses in broad beam configuration. Lateral dose profiles at surface and 20 mm of depth. The values were normalized to the maximum value.

By using the validated source model, the dose distributions in both the homogeneous and heterogeneous solid phantoms were assessed. Figure 3 depicts the FWHM of the central peak of the MBRT array in the homogeneous configuration. A good agreement is observed between MC and experimental data. The FWHM at the entrance is 618 $\pm$ 18 μm, equal to the one at synchrotrons, 630 $\pm$ 50 μm [1], within the uncertainty bars. Due to the large divergence, the FWHM will increase up to 1000 μm at 40 mm of depth, in contrast to synchrotrons, where the FWHM stays almost constant as a function of depth. The MC beam patterns reproduce well the experimental values in both the homogeneous [6] and heterogeneous phantoms (see figure 4 (a) and 4 (b), respectively)), according to the criteria explained in the TRS430 [9]. At a depth of 30 mm, the differences reach the critical value of 3% (see figure 4 (a)). However, at this depth, this is already outside the head of the animal (see figure 6). The centre-to-centre (ctc) values between the three central peaks at a depth of 10 mm are 1465 $\pm$ 10 μm and 1478 $\pm$ 15 μm for experimental and MC respectively.

Table 1 compares the PVDR values at the ESRF [2] with the ones obtained in this research. The experimental and calculated values are in agreement. In both the synchrotron and SARRP systems, the PVDRs in the entrance are very high. The PVDR then decrease. But, while the PVDR remain constant as a function of depth in the case of the synchrotron, a continuous decrease is observed in the SARRP due to the significant beam divergence.

The output factors (OF) for the central peak were calculated with respect to the broad beam (40 x 40 mm^2 field size). Table 2 shows the experimental and theoretical values of the OF. A good agreement is also found. The OF decrease by a factor of 3

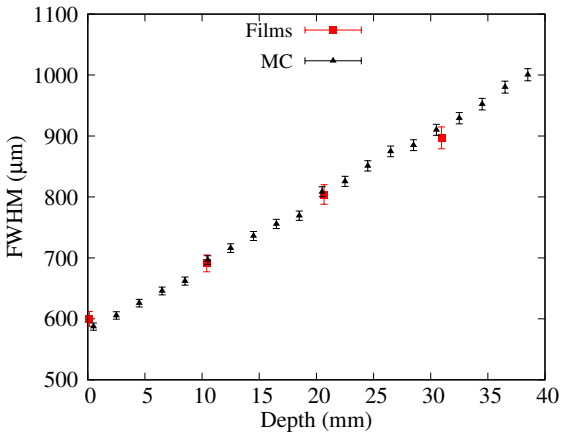

Figure 3: Full width at half maximum of the central peak, comparison between experimental (red square) and MC (black triangles).

Table 1: PVDR at different depths obtained experimentally from synchrotron [2] and experimentally using Gafchromic films and MC simulations in this research. The acronyms are as follows: this-w-ho: This work, homogeneous phantom and this-w-he: This work, heterogenous phantom.

Depth (mm)	Sync-MBRT film	this-w-ho [6] film	this-w-ho MC	this-w-he film	this-w-he MC
Surface	21.7 ± 2.2	27.8 ± 2.8	25.4 ± 1.3	24.5 ± 1.4	24.3 ± 1.5
10	17.5 ± 1.8	12.4 ± 2.3	11.6 ± 0.9	10.1 ± 0.7	9.1 ± 0.6
20	16.1 ± 1.6	9.4 ± 2.0	7.8 ± 0.5	7.1 ± 0.6	6.2 ± 0.4
30	15.6 ± 1.6	7.0 ± 1.8	5.4 ± 0.3	5.7 ± 0.5	5.2 ± 0.3

when moving from the entrance to a depth of 3 cm. That is to say, at the surface the dose deposited by the central peak of the array is 9% lower than the one deposited by a 40 x 40 mm^2 field size, while at a depth of 3 cm, the dose in the peak is 67% lower than in broad beam conditions, due to lateral scattering and beam divergence.

The validated dose-engine was employed to calculate the dose distributions in the voxelized rat phantoms with the objective of planning the in vivo experiment. First of all, the dose-engine was calibrated. The experimental dose at a depth of 10 mm in the solid water phantom was compared with the calculated dose at the same depth (reference dosimetry conditions). Taking into account the number of primary particles in the simulation, a correlation of the dose at the centre of the rat can be established

Table 2: Output factors obtained experimentally by using Gafchromic films and theoretically by MC simulations.

Depth (mm)	OF (film)	OF (MC)
Surface	0.91 ± 0.04	0.92 ± 0.08
10	0.62 ± 0.02	0.63 ± 0.05
20	0.45 ± 0.02	0.47 ± 0.03
30	0.33 ± 0.01	0.35 ± 0.02

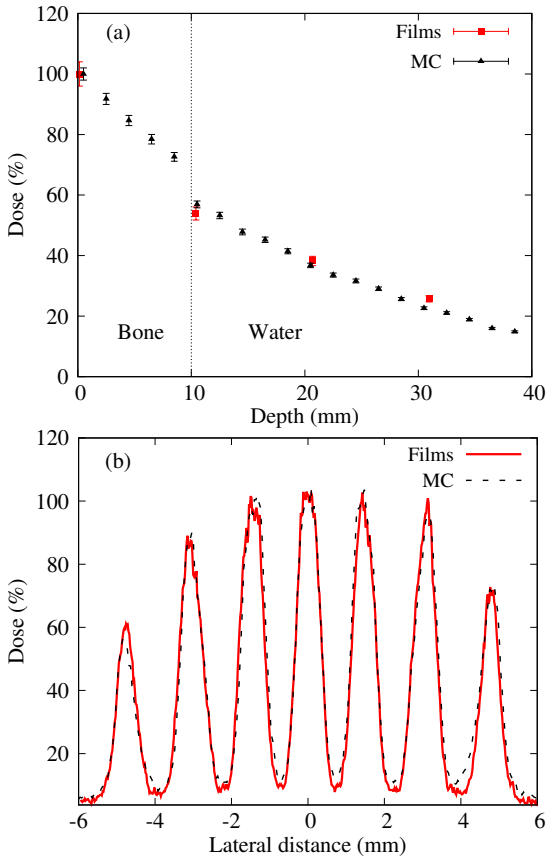

Figure 4: Dose distributions in the heterogeneous phantoms (bone 10 mm + water), comparison between experimental (red square) and Monte Carlo (black triangles) dosimetry. Percentage depth dose, panel (a) and lateral dose profiles at 10 mm of depth, panel (b) . The values were normalized to the maximum value of the central peak.

with respect to the dose at the reference conditions. The latter amounted to 66% ± 1% of the dose at the reference conditions.

The dose distribution profiles at the centre of the rat brain (13.6 mm depth) and at the tumor location (16 mm depth) were compared between CT and ROBY phantoms, see figure 5. A good match was reached except that differences of up to 20% are obtained in the most extreme peak (-5 mm in the y axis figures 5 and 6) where the thickness of the bone in the ROBY phantom is almost 2 mm in contrast to 1 mm in the CT. Using the ROBY phantom, it is not necessary to make a CT scan for each animal for planning purposes, which leads to economic savings, since it is possible to adapt the parameters of the ROBY phantom taking into account the age of the animal. The PVDR values obtained for the CT and ROBY at a depth of 13.6 mm were 9.0 ± 1.3 and 9.2 ± 1.2 respectively and at a depth of 16 mm, they were 8.2 ± 1.3 and 8.5 ± 1.2 respectively. These values were used to estimate the doses at the centre and at the location of the

tumor. The doses calculated using the dose-engine program at the approximate centre of the tumor (16 mm depth) were 33.2 ± 1.7 Gy and 4.0 ± 0.4 Gy, peak and valley, respectively, when the CT images are used and 34.2 ± 1.7 Gy and 4.0 ± 0.4 Gy, peak and valley doses, when using the ROBY phantom. The average dose at a depth of 16 mm was 14.2 ± 0.9 Gy and 13.6 ± 0.8 Gy, in the CT and ROBY, respectively.

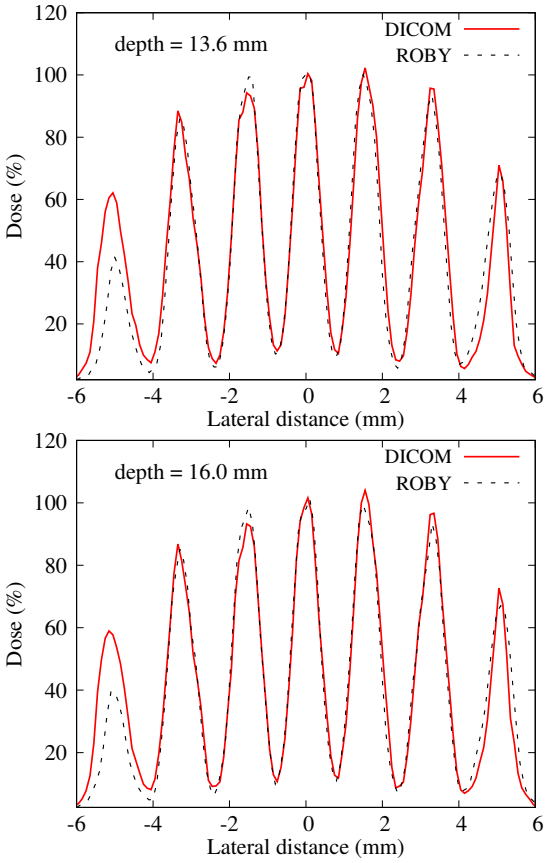

Figure 5: Lateral dose profiles at the centre of the rat brain (13.6 mm depth, left panel) and at the position of the tumor (16 mm depth, right panel). The values were normalized to the maximum value of the central peak.

3.2. In vivo experiment

Figure 7 shows the survival curve obtained in the in vivo experiment with the male Fisher rats. The median survival time post-implantation was calculated (28 days for the controls versus 35 days for the irradiated animals). Kaplan Meier survival data were plotted versus time after tumor implantation. The survival curves were compared using the log-rank test between the irradiated group and the controls (Prism-GraphPad). The two curves are statistically significantly different ($p = 0.0017$). The histological analysis confirmed the presence of tumors in all animals.

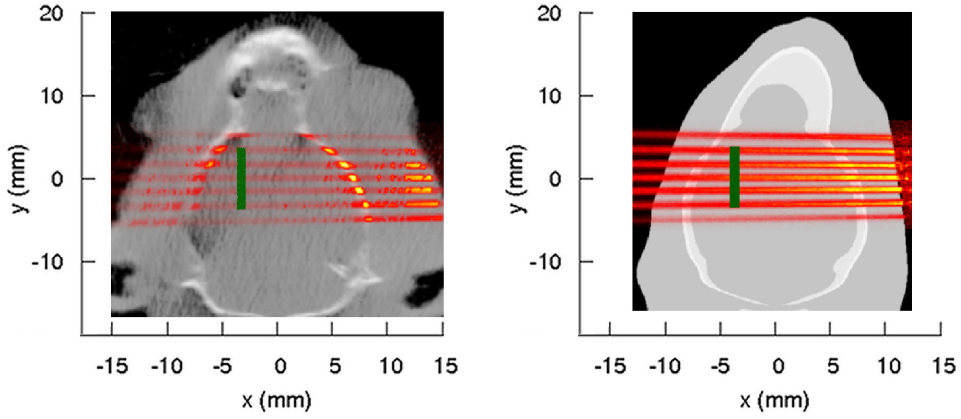

Figure 6: Coronal view of the dose distributions overlapped with the mass density maps for a CT slice (left panel) and for a ROBY slice (right panel). The location of the tumor is represented by a green line.

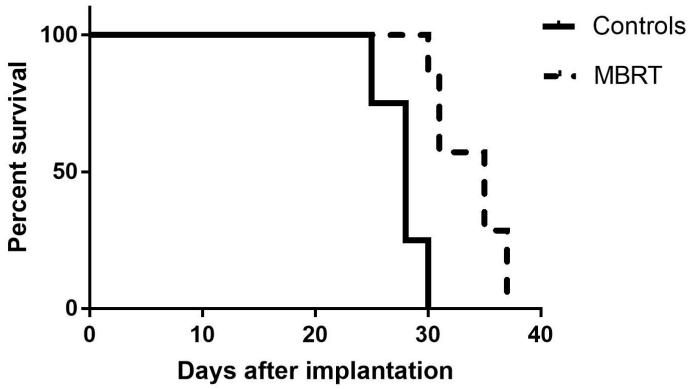

Figure 7: Survival curves of the control and irradiated groups. MBRT treatment resulted in a statistically significant but modest increase of mean survival time with respect to the untreated controls.

4. Discussion

Minibeam radiation therapy is a promising radiotherapy technique whose advancement has been hindered due to the limited beamtime access at large synchrotrons. We have recently shown the feasibility of transferring this technique to a small-animal irradiator [6]. In contrast to some other work [18, 19], our implementation allows the irradiation of intracranial tumors in rodents, as has been shown in the present technical note. Therefore, our system offers the possibility of performing systematic and comprehensive radiobiological experiments to investigate the distinct biological effects that occur when a spatial fractionation of the dose is used.

To guide such experiments, reliable dosimetry tools are needed to be able to extract

valid conclusions. This includes a dose-calculation engine. With that aim, we have performed a series of experimental measurements both in homogeneous and heterogeneous dose phantoms. These measurements confirm that our beam patterns are similar to those at synchrotrons: similar beam widths, ctc distances and PVDR were obtained. In addition, they served to benchmark the preclinical dose-calculation engine that we have developed. To gain in calculation efficiency, we determined a virtual source model, that was subsequently used as beam source in the dose-calculation engine.

Finally, we have used the developed tools to evaluate the dose distributions delivered to a series of F98 tumor-bearing rats. Unlike other MBRT table-top solutions [18, 19], our system allows the irradiation of intracranial tumors in rodents, as has been shown in the present technical note. Following our previous paper [6], demonstrating that normal rats do not exhibit any important brain damage after an MBRT irradiation with a 58 Gy peak dose, the pilot experiment reported here aimed at assessing whether this dose prescription was also enough to achieve some **tumor response**. A modest but statistically significant increase of mean survival time was observed in the treated group with respect to the controls. No comparison was possible with standard broad beam conditions, as the prescribed dose would not have been well tolerated [6].

5. Conclusions

This technical note reports on the dosimetric tools that we have developed to reliably guide preclinical trials in a table-top MBRT system. As a proof of concept, we have performed a pilot experiment of the treatment of intracranial glioma-bearing rats. The increase in mean survival life due to the treatment of intracranial glioma-bearing rats is small but statistically significant. However, the fact that normal tissues are able to withstand the high doses employed in this study, in contrast to conventional irradiation, opens the possibility of escalating the dose in the tumor and the use of interlaced or cross-fired geometries to improve the treatment's outcome.

Acknowledgments

This research was performed with financial support from ITMO Cancer AVIESAN (Alliance Nationale pour les Sciences de la Vie et de la Santé, National Alliance for Life Sciences and Health) within the framework of the Cancer Plan (2009–2013), under grant agreement PC201327. The authors acknowledge the calculation time provided at Centre de Calcul de Lyon (IN2P3), at Grand Equipement National de Calcul Intensif (in particular at the supercomputer Curie of CEA) and PRACE for awarding us access to the MareNostrum computational cluster at BSC (Spain) under grant agreement number 2016153507.

Reference

[1] Prezado Y, Renier M and Bravin A. A new method of creating minibeam patterns for synchrotron radiation therapy: a feasibility study. J Synchr Radiat 2009;16:582-6.

[2] Prezado Y, et al. Dosimetry protocol for the preclinical trials in white-beam minibeam radiation therapy. Med Phys 2011;38:5012-20.

[3] Dilmanian FA, Button TM, et al. Response of rat intracranial 9L gliosarcoma to microbeam radiation therapy. Neuro Oncol 2002;4:26-38.

[4] Prezado Y, Deman P, et al.. Tolerance dose escalation in minibeam radiation therapy applied to normal rat brain: long-term clinical, radiological and histopathological analysis. Rad Research 2015;184:314-2.

[5] Prezado Y, Sarun S, et al. Increase of lifespan for glioma-bearing rats by using minibeam radiation therapy. J Synchr Radiat 2012;19:60-5.

[6] Prezado Y and dos Santos M, González W, et al. Transfer of Minibeam Radiation Therapy into a cost-effective equipment for radiobiological studies: a proof of concept. Sci Rep 2017;7:17295.

[7] http://www.xstrahl.com/

[8] Agostinelli S, et al. Geant4 a simulation toolkit. NIM A 2003;506:250-303.

[9] International Atomic Energy Agency 2004 Commissioning and quality assurance of computerized planning systems for radiation treatment of cancer IAEA Technical. Report Series 430 (Vienna: IAEA) 2004.

[10] *http : //www.sunnuclear.com/solutions/machineqa/solid_water_he*

[11] Keenan MA, et al. RADAR Realistic Animal Model Series for Dose Assessment. J Nucl Med 2010;51:471-6.

[12] Hamdia M, et al. Impact of X-ray energy on absorbed dose assessed with Monte Carlo simulations in a mouse tumor and in nearest organs irradiated with kilovoltage X-ray beams. Cancer Radiother 2017; 21:190-8

[13] Reynaert N, et al. Monte Carlo treatment planning for photon and electron beams. Radiat Phys Chem 2007;76:643-86.

[14] Devic S, et al. Precise radiochromic film dosimetry using flat-bed document scanner. Med Phys 2005;32:2245-53.

[15] Niroomand-Rad A, et al. Radiochromic film dosimetry: Recommendations of AAPM Radiation Therapy Committee Task Group 55. Med Phys 1998;25:2093-115.

[16] Sorriaux J, et al. Evaluation of Gafchromic EBT3 films characteristics in therapy photon, electron and proton beams. Phys Med 2013;29:599-606.

[17] Prezado Y, et al. Proton minibeam radiation therapy widens the therapeutic index for high-grade gliomas. Sci Rep 2018;8:16479.

[18] Bartzsch S, et al. preclinical microbeam facility with a conventional x-ray tube. Med Phys 2016;43:6301-08.

[19] Bazyar S, et al. Minibeam radiotherapy with small animal irradiators; In vitro and in vivo feasibility studies. Phys Med Biol 2017;62:8924-42.